

Note to Readers: Some or all of the figures in this paper may have been scanned or prepared at screen resolution for optimal online viewing. When printed, the quality of these figures may be inferior to those that appear in the printed journal. The page numbers begin with one, and do not correspond to the page numbers that appear in the printed journal, which has a different layout. The printed version of this paper is available in PDF format on the *Advances in Environmental Research* web site at <http://www.sfo.com/~aer> (Volume 1, Number 2).

## **SEDIMENT-TO-AIR MASS TRANSFER OF SEMI-VOLATILE CONTAMINANTS DUE TO SEDIMENT RESUSPENSION IN WATER**

K. T. Valsaraj <sup>\*1</sup>, R. Ravikrishna <sup>1</sup>, J. J. Orlins <sup>2</sup>, J. S. Smith <sup>1</sup>, J. S. Gulliver <sup>2</sup>,  
D. D. Reible <sup>1</sup> and L. J. Thibodeaux <sup>1</sup>

<sup>1</sup>Department of Chemical Engineering, Louisiana State University, Baton Rouge, LA 70803

<sup>2</sup> St. Anthony Falls Laboratory, Department of Civil Engineering,  
University of Minnesota, Minneapolis, MN 55455

\*Corresponding author. Phone: (504) 388-1426, Fax: (504) 388-1476, E-mail: [kvalsar@lsuvm.sncc.lsu.edu](mailto:kvalsar@lsuvm.sncc.lsu.edu)

### **ABSTRACT**

Experiments were conducted to determine air emissions of semi-volatile organic compounds (SVOCs) from a contaminated bed sediment resuspended in the water column such as occurs in a confined disposal facility (CDF) immediately after dredging and storage. A local sediment (University Lake, Baton Rouge, LA) was inoculated with three SVOCs (dibenzofuran, phenanthrene and pyrene). A grid-stirred tank was fabricated that generated uniform turbulence at the sediment surface to give the desired suspended sediment concentration in the water. Sediment resuspension was related to the turbulence near the sediment-water interface which was characterized by the Hopfinger-Toly relationship. The flux of the SVOCs to the air was measured at various suspended sediment concentrations and was found to vary in the order dibenzofuran > phenanthrene > pyrene. The flux increased with increasing suspended sediment concentration in water, increasing Henry's constant and decreasing sediment/water partition constant for the chemical. The overall mass transfer coefficients showed significant gas phase resistance for the SVOCs. The implications for assessing air emissions from a CDF are discussed.

*Keywords: air emission flux, semi-volatile organic compounds, resuspended sediment*

## INTRODUCTION

Contaminated sediment and dredged material can be sources of emissions of volatile and semi-volatile compounds to the atmosphere. At present neither sufficient field data nor verified models exist to accurately predict these emissions under different conditions. A literature review of the various pathways of air emissions from dredged materials stored in a confined disposal facility (CDF) was performed [1]. There are few reports of studies in which air emissions have been monitored near a dredge head or near a CDF. At the New Bedford Harbor, Massachusetts site where an ambient air monitoring program was initiated to evaluate the impact of dredging and storage of contaminated sediments, significant air emission of polychlorinated biphenyls (PCBs) was noted during dredging of “hot-spots” and operational changes were made to reduce emissions [2]. Van Oostrum and Vroege [3] observed that for contaminant dredging to be operationally viable, one needs to pay particular attention to the minimization of contaminant release to the water column from resuspended sediments.

The resuspension of sediments and uncontrolled release of contaminants are considered negative aspects of dredging and remediation of contaminated sediments. During the dredging and filling of a CDF, inevitably a portion of the sediment is released to the water column. Upon resuspension, whether near the dredge-head or in ponded water in a CDF, contaminants originally within the sediment come in contact with water that contains little or no contaminant. The driving force for mass transfer is favorable for desorption of contaminant into the water. Contaminants in the water column are then available for volatilization into the atmospheric boundary layer above the water column. The extent of desorption determines the availability of compounds in the aqueous phase for volatilization. Figure 1 shows the distribution of a contaminant between the various phases in a CDF or near a dredge head. There are several important questions relating to the fate and transport of resuspended particles and contaminants [3]. Primarily we need to know how much of the contaminant is released to the water column and to the atmosphere, and for how long is there a substantial release rate after the filling of a CDF? The research presented here is directed towards providing the data required to answer the above questions.

In natural systems, sediment resuspension is driven by turbulent shear stresses at the sediment-water interface. Resuspension does not occur in any significant quantity unless the bed shear is above a critical value. One way to simulate this process is with an oscillating grid turbulence generator. Oscillating grids have been used since the 1950's to develop nearly isotropic, laterally homogeneous turbulence on a small scale, without the mean shear associated with water flowing over a surface. Numerous investigators have used these grids to study topics such as mixing across density interfaces [4, 5], turbulence near an air-water interface [6], sediment resuspension [7, 8] and desorption of contaminants from sediments [9]. Chu

and Jirka [6] used a 50 cm x 50 cm square tank with an oscillating grid of mesh size 6.36 cm to study the aqueous-phase controlled transport of oxygen at the air/water interface. Tsai and Lick [7] used a small, portable device to determine the resuspension potential for cohesive sediments in the field. Huppert *et al.* [8] studied the entrainment of non-cohesive sediments using an oscillating grid. Connolly *et al.* [9] used an oscillating grid reactor to study the desorption of Kepone (a hydrophobic chemical) from natural sediments to water.

The aim of the current project was to develop a device for resuspending cohesive sediments in a controlled manner and to measure the resulting flux of compounds from sediment to the atmosphere. The well-established body of literature described above provided the basis for selecting an oscillating grid

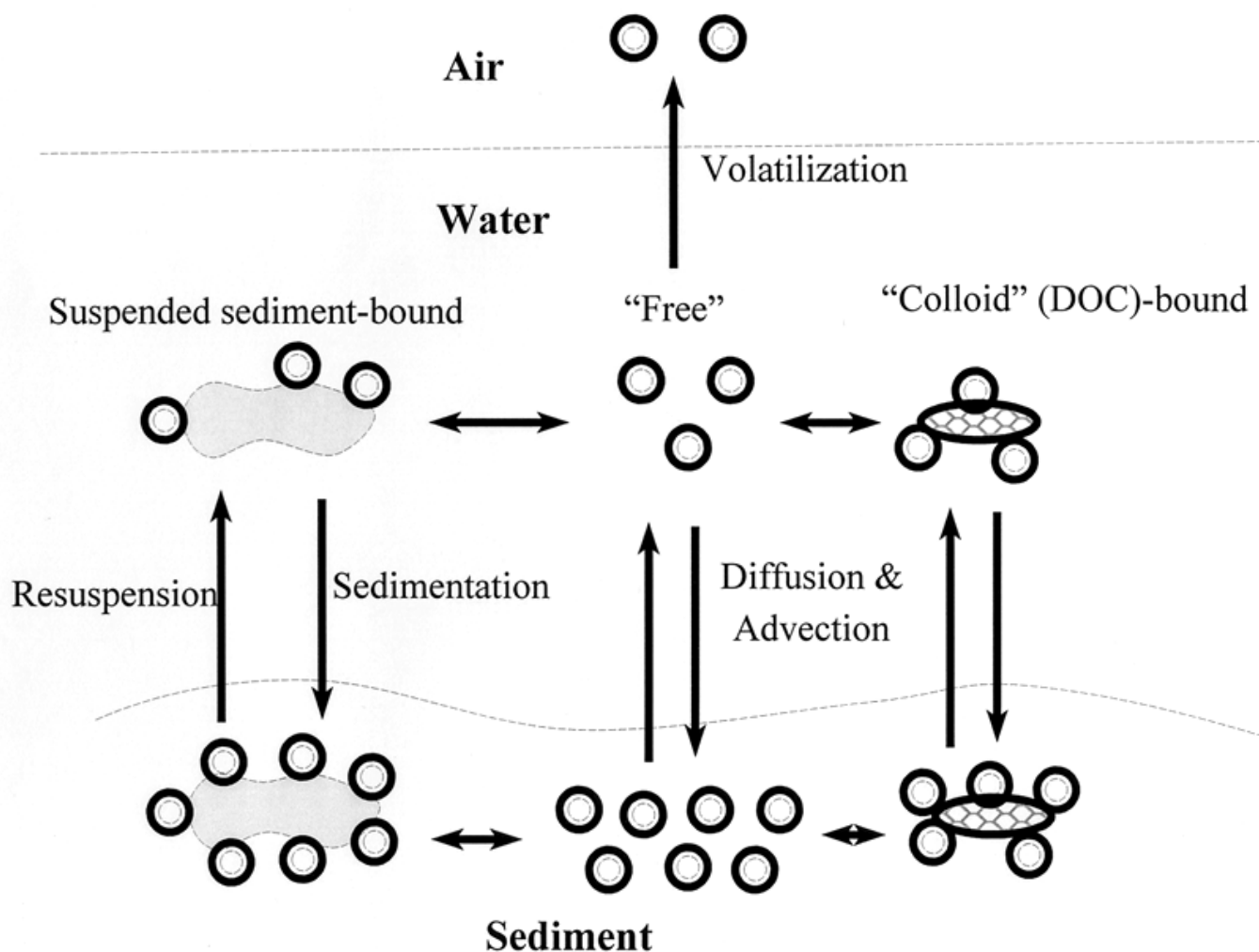


Figure 1. A schematic of the distribution of contaminants resulting from resuspension of a contaminated sediment bed.

mechanism to generate shear-free turbulence to resuspend the sediments. However, no previous work has been done on linking all of the aspects mentioned above (sediment resuspension  $\Leftrightarrow$  turbulence  $\Leftrightarrow$  air-water mass transfer) together in one experimental setup. Consequently, each of the processes or mechanisms must be verified against results reported in the literature for the sediment resuspension/chemical flux chamber developed for this project.

We focused our attention on the release of several semi-volatile organic compounds, namely, pyrene (PYR), phenanthrene (PHE) and dibenzofuran (DBF) from a local cohesive sediment (University Lake, Baton Rouge, LA) that was spiked with the chemicals of concern. Different levels of sediment resuspension were achieved in the grid-flux chamber and the sediment concentrations related to the total kinetic energy imparted to the sediment. The turbulence in the chamber was quantified using a laser doppler velocimeter system. Sediment-to-air flux and water concentrations of the organic chemicals were measured and mass transfer coefficients to air estimated and interpreted.

## **EXPERIMENTAL**

### *(a) Flux Chamber*

A square chamber was chosen for construction and to make use of the well-developed theory of oscillating grid turbulence. A large plan-form area was desired to facilitate measuring chemical fluxes across the air-water interface. The chamber was manufactured out of clear, acrylic plastic, as shown in Figure 2. The chamber was a cube 50 cm on each side, with a tight-fitting lid. The grid consisted of an 8 x 8 mesh made out of 1.27 cm square aluminum bars, with a center-to-center spacing of 6.25 cm, and a bar length of 49 cm. The grid was connected to a 0.25 kW variable speed DC motor by a stainless steel shaft and eccentric drive. A steel frame supported the drive motor and was permanently fastened to the lid. An acrylic guide was fastened to the back wall of the tank and prevented the grid from rotating in the tank. The grid stroke length could be adjusted from 2 to 12 cm by changing the pin location of a connecting rod between the vertical shaft and eccentric drive. The oscillation frequency was set and maintained by a closed-loop programmable controller. Frequencies from 60 to 600 rpm (1 to 10 Hz) could be maintained, depending on the stroke length. Sediment was placed in the bottom of the chamber by removing the grid/lid/frame assembly. Water samples were removed from the tank via a sampling port in the lid of the tank

and side-ports.

*(b) Experimental Setup*

The inlet house air was pulled through 5 g of 4-12 mesh activated carbon (Aldrich Chem. Co., St. Louis, MO) trap before introduction into the chamber. Air flow rates of 12 L/min and 24 L/min were used in the experiments. The air was pulled from the grid-flux chamber using a vacuum pump (VWR Scientific, West Chester, PA, 0.25 kW). The outlet air was filtered through a trap (1-2 g of XAD-2 resin, Supelco Inc., Bellefonte, PA) kept in place in a glass tube with glass wool plugs at both ends. A thermometer introduced through the lid indicated the air temperature.

*(c) Experimental Procedure*

Contaminated sediment was placed in the chamber and spread evenly to a depth of 5 cm. After consolidation for a period of time, samples were collected from the surface sediment for polyaromatic hydrocarbon (PAH) analysis. Water was then added slowly through a small tube placed parallel and close

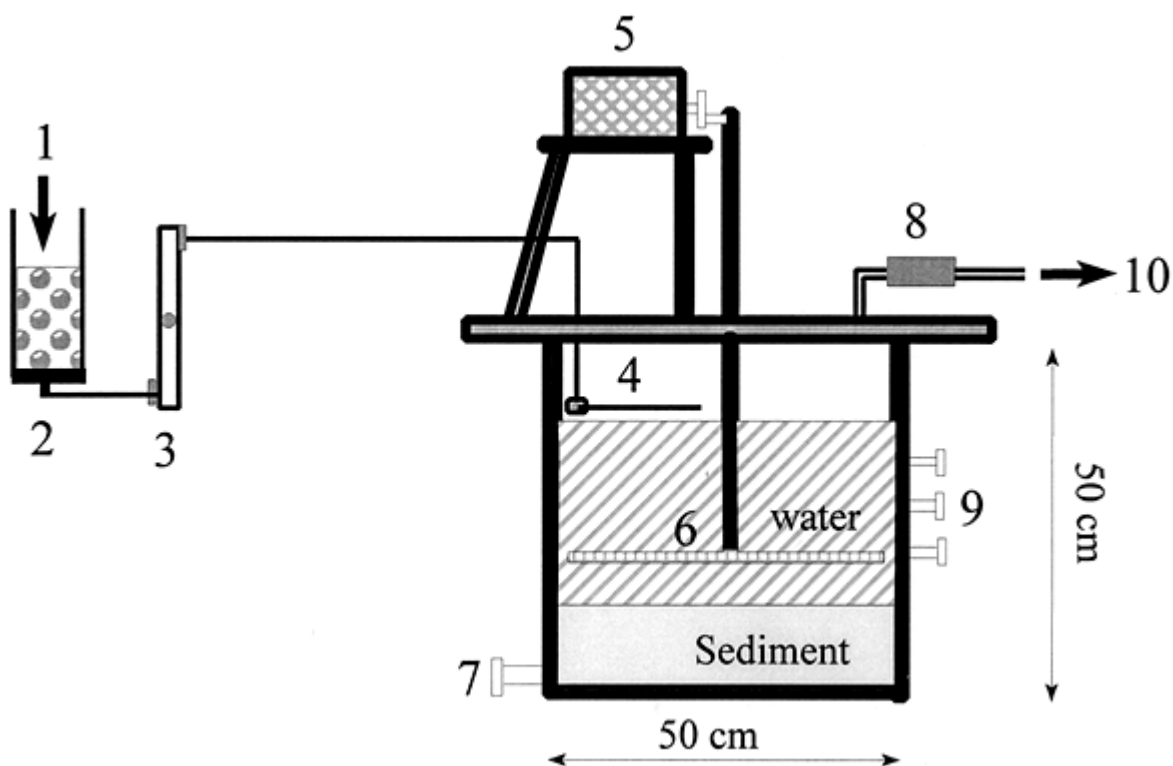


Figure 2. Schematic of set-up for air emission measurement: 1- house air inlet, 2- activated carbon trap, 3- rotameter, 4- air inlet and distributor, 5- motor (0.25 kW), 6- grid assembly, 7- outlet port, 8- XAD resin trap, 9- sampling port for water, 10- air outlet to hood.

to the sediment in such a manner as not to resuspend any of the sediment. The lid/frame assembly was carefully placed back on the chamber and secured tight.

Air samples were obtained within a particular time interval on the adsorbent placed in the trap at the exit. The trap was placed at the beginning of a sampling interval and replaced at the beginning of the next interval. An aqueous sample is one collected through the lowest port at the end of the sampling interval. A blank is the set of air and water samples collected without any grid stroke, i.e, no external kinetic energy input. The free vapor space above the water level was flushed out by flowing air through the chamber for a time approximately equaling two residence times. This was done to ensure that the blank values of flux to air represented the true blank values and not the stagnant PAHs that might have collected in the vapor space during the sediment consolidation period. Before the grid stroke was started, one set each of blank air and water sample was collected.

An experimental run was deemed to have begun when the grid stroke began. A stroke length of 4 cm and frequencies of 2 to 5 Hz were used to obtain different degrees of kinetic energy input. The height of the water column was 40 cm from the bottom of the chamber. The elevation of the grid center of motion from the bed was 8.5 cm.

### *(c) Sediment and Tracers Used*

The sediment used was from a local lake (University Lake, Baton Rouge, LA). Uncontaminated sediment samples were obtained from the lake using box corers. The sediment was subsequently processed by sieving through a coarse sieve to remove rocks and other debris. It was then homogenized and stored in plastic containers for use. The relevant properties of the sediment are given in Table 1. The sediment is cohesive in nature.

Pyrene, phenanthrene and dibenzofuran were used as tracers in the sediment. Dibenzofuran, although a heterocyclic aromatic compound, has properties similar to the two other PAHs and was analyzed in the same way as the PAHs. All three chemicals are classified as semi-volatile and have low vapor pressures and aqueous solubilities. They are all highly hydrophobic as indicated by their large octanol-water partition constants. They are also prevalent at many contaminated sediment sites in the United States. Table 1 lists the properties of the chemicals used.

To contaminate the sediment uniformly with the PAHs, a well established method was used [10].

The sediment loadings were determined after this procedure and are given in Table 1.

*(d) Sample Treatment, Extraction and Analyses*

The sediment samples collected after the consolidation period were extracted by the following procedure. One gram of sediment was weighed into a 100 mL bottle and 10 g of anhydrous sodium sulfate was added and thoroughly mixed before adding 60 ml of 1:1 hexane/acetone mixture. The samples were sonicated for 30 minutes and then allowed to settle for a few hours.

The contents of the PAH trap (from the air samples) were transferred to a bottle, and 40 mL methylene chloride added. The bottle was tightly capped and placed in an ultrasonic bath for 30 minutes at room temperature.

Table 1. Properties of the Sediment and Contaminants.

Sediment Properties			
sand (% g/g)		3	
silt (% g/g)		41	
clay (% g/g)		56	
Fraction organic carbon ( $f_{oc}$ , g/g)		0.03	
Bulk density ( $g/cm^3$ )		0.67	
Total porosity, (-)		0.7	
Contaminant Properties at 298 K* and Concentrations			
	DBF	PHE	PYR
Molecular weight	168	178	202
Sediment loading (mg/kg)	$66 \pm 4$	$65 \pm 5$	$69 \pm 4$
Water solubility (mg/L)	10	1	0.15
$\log K_{oc}$ (L/kg)	4.0	4.4	4.8
$\log K_{ow}$	4.1	4.5	5.1
Henry's constant, $H_c$ (-)	$2.4 \times 10^{-3}$	$9.8 \times 10^{-4}$	$4.5 \times 10^{-4}$
Vapor pressure (mm Hg)	$3.6 \times 10^{-3}$	$2.5 \times 10^{-4}$	$4.5 \times 10^{-6}$
Diffusivity in water ( $cm^2/s$ )	$6.0 \times 10^{-6}$	$5.8 \times 10^{-6}$	$5.5 \times 10^{-6}$
Schmidt number, $Sc_{Aw}$	1666	1724	1818

\*All values are from Thoma [10].

100 mL of aqueous sample was used for the determination of total suspended solids (TSS) and dissolved organic carbon (DOC) in water. TSS in water was measured using the Standard Method 2540D [11]. The glass fiber filter used for this purpose had a 1  $\mu\text{m}$  pore size (Poretics, Livermore, CA). The filtrate from the TSS analysis was collected for DOC analysis using Standard Method 505A [11] using a Shimadzu TOC-500 instrument.

A 400 mL aqueous sample was used for PAH analysis. The analysis of the unfiltered aqueous sample yielded the total concentration of PAHs in the aqueous phase which included that associated with the TSS. It was mixed with 40 mL hexane, shaken for 25 min and sonicated for a few minutes to accelerate the separation of the aqueous and hexane phases.

The solvent phases (from the PAH trap for the air sample and the extract for the water sample) were transferred into 20 mL vials and concentrated to about 2 mL by nitrogen blowdown. They were then transferred to a 2 mL volumetric tube and further concentrated to 0.2 mL. Acetonitrile was added to make up the volume to 2 mL. The acetonitrile sample was then analyzed for the PAHs using Standard EPA Method 8310 [12]. The analysis was carried out on a Hewlett Packard 1090L liquid chromatograph using a 60:40 mixture of acetonitrile and water as the mobile phase. The column used was Envirosep-PP (Phenomenex, Torrance, CA).

*(e) Data Reduction*

The flux to air,  $N_A$  ( $\text{ng}/\text{cm}^2 \cdot \text{h}$ ), was calculated from the total PAH captured in the trap,  $\Delta m_A$  (ng), during the duration  $\Delta t$  (h).  $N_A = \Delta m_A / (\Delta t \cdot A)$ , where  $A$  is the air-water interface area in the tank ( $= 2500 \text{ cm}^2$ ). The aqueous concentration measured is the total dissolved PAH concentration,  $\rho_{Aw}^t$ . A correction was applied to the PAH associated with the unfilterable DOCs and suspended solids using the factor  $(1 + \rho_s K_d + \rho_{DOC} K_{DOC})$ . Thus the “free” dissolved PAH in water is  $\rho_{Aw} = \rho_{Aw}^t / (1 + \rho_s K_d + \rho_{DOC} K_{DOC})$ , where  $\rho_s$  is the concentration of suspended solids in water (kg/L),  $\rho_{DOC}$  is the DOC concentration (kg/L),  $K_d$  is the sediment-water partition constant (L/kg),  $K_{DOC}$  is the DOC-water partition constant (L/kg) and  $\rho_{Aw}^t$  is the total PAH concentration (kg/L) obtained by extraction of the whole sample.  $K_d$  was obtained from a knowledge of the organic-carbon based partition constant,  $K_{oc}$ , and the fraction of organic carbon in the sediment. For the dissolved organic carbon, we assumed  $K_{DOC} \approx K_{oc}$ .

## RESULTS AND DISCUSSION

Before using the grid chamber for air emission flux measurements, it was deemed important to demonstrate that the degree of resuspension was uniform, and that a steady state was achieved in a short time. It was also necessary to show that the size distribution of suspended solids in the water column spanned a narrow range. Hence, a series of tests was conducted to determine the relationship between suspended solids and turbulence generated by the oscillating grid. The total mass of suspended solids was measured as a function of oscillation frequency, stroke length and consolidation time. Several tests were run, with frequencies of 150 to 650 rpm (2.5 to 10.8 Hz), strokes of 2, 3 and 4 cm, and consolidation times of 2 to 24 days. The initial elevation of the sediments in the tank for this series of tests was typically 5 to 10 cm, and the water level was 20 to 35 cm. The grid was adjusted to the desired stroke length, and positioned so that its center of motion was either 8.5 cm or 12.5 cm above the bed. For each test, the grid was oscillated at its lowest frequency, and water samples were withdrawn at regular intervals for analysis. The time-history of suspended sediment concentration for a representative test showed that a steady state concentration within measurement uncertainty was achieved in 10 to 30 minutes for each case [13]. For later tests, the oscillation frequencies were maintained for at least 30 minutes before being increased.

Since there is no mean shear in an oscillating grid mixing chamber, the total kinetic energy ( $E_k$ ) of turbulence provides a basis for comparing sediment suspension and mass transfer under differing operating conditions. Using the Hopfinger-Toly relationship [5], the following equation can be derived

$$E_k = \alpha (MS^3f^2z^{-2}) \quad (1)$$

where  $\alpha$  is 0.082 [15],  $M$  is the mean mesh spacing of the grid (= 6.25 cm),  $S$  is the stroke length (cm),  $z$  is the distance away from the virtual origin (= 8.5 cm) and  $f$  is the frequency of the stroke ( $s^{-1}$ ).  $E_k$  is in  $cm^2/s^2$ . A virtual origin is obtained by extrapolation of the integral scale to zero. It is, for all practical purposes, identical to the mid-plane of grid oscillation. We quantified turbulence in the mixing chamber using a two-component laser doppler velocimeter (LDV) system manufactured by TSI of St. Paul, MN. The details of the measurement are given elsewhere [13]. The LDV system was configured to measure velocities in the coincidence mode and allowed direct computation of the Reynolds stress,  $\overline{uw}$ , where  $u$  and  $w$  are

instantaneous velocity fluctuations in the horizontal and vertical directions. It was also possible to measure the individual root mean square (RMS) velocities,  $u'$ ,  $v'$ , and  $w'$  which allowed the value of  $E_k = 0.5 (u'^2 + v'^2 + w'^2)$  to be computed. The measured values were found to compare favorably to the predictions of Equation (1), thus lending credence to the use of the Hopfinger-Toly relationship to characterize turbulence in the mixing chamber. Figure 3 displays the relationship between the observed total suspended solids concentration ( $\rho_s$ ) and the corresponding value of  $E_k$  estimated using Equation (1). As can be seen from the figure, the suspended sediment concentrations ranged from 0.01 to 3 g/l.

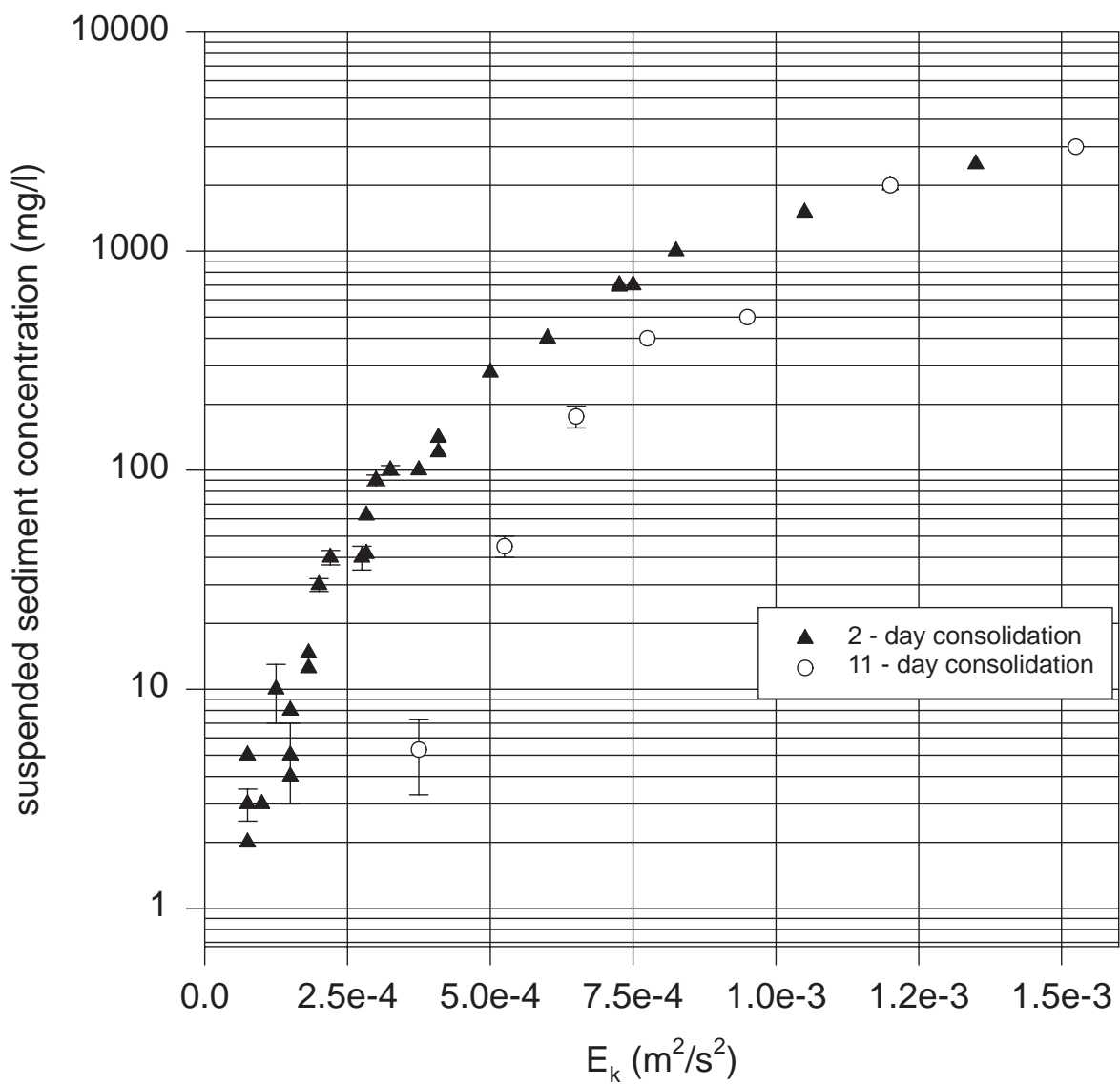


Figure 3. Suspended sediment concentration versus total kinetic energy imparted by the oscillating grid.

Consolidation is the term used to describe an in-bed process that occurs once the particles arrive on the bottom. In a natural setting, such as occurred in the test apparatus with saturated sediment, the individual particles arrange themselves in conjunction with each other in a compact form expelling water up as they do so. This results in a tighter packing arrangement and a bed with less porosity. Consolidation changes occur rapidly in the first few days and less so as time passes. The net effect is a bed of particles with more contact points for cohesion to occur which in turn resists resuspension. Figure 3 indicates a distinct difference in resuspension concentration for sediment allowed to consolidate for 11 days as opposed to 2 days.

The size distribution of suspended particles in the water phase was determined using an Elzone particle size distribution analyzer. Geometric mean particle sizes ranged from 10 to 14  $\mu\text{m}$  with an average size of 11.7  $\mu\text{m}$ . Geometric standard deviations ranged from 1.7 to 2  $\mu\text{m}$  with an average of 1.8  $\mu\text{m}$ . The mean size was found to be independent of the grid oscillation frequency or sediment consolidation time. The uniformity of the suspended material under different operating conditions could be due to either the homogeneity of the sediment or some mechanism which breaks down larger flocculated particles. Such mechanisms could include the turbulent shear associated with flocs passing through the oscillating grid. The uniformity in size is particularly significant since recently it has been shown that for suspended particles in water the characteristic time for desorption varies with particle size [14]. Consequently, the concentration in the water column will also vary and hence influence the flux to air. In our experiments, the homogeneity of suspended particles negated any size-dependent effects on the air emission flux. We also observed that the suspended sediment concentration was uniform throughout the water column. For example, at an  $E_k$  value of 4  $\text{cm}^2/\text{s}^2$ , we obtained suspended sediment concentrations of  $362 \pm 22$ ,  $362 \pm 1$  and  $350 \pm 3$   $\text{mg/l}$ , respectively at distances 10, 20 and 30 cm above the sediment surface. The uniformity of suspended sediment concentration also allows us to assume a single partition coefficient to represent the equilibrium between the suspended solids and the water column.

The overall flux of a contaminant from water to air is given by

$$N_A = K_{Aw} \left( \rho_{Aw} - \frac{\rho_{Aa}}{H_c} \right) \quad (2)$$

where  $\rho_{Aa}$  is the air phase concentration of contaminant A and  $H_c$  is the Henry's constant ([mol/L]/[mol/L]).  $K_{Aw}$  is the overall aqueous phase mass transfer coefficient for chemical A (cm/s). The water concentration is the "free" water concentration that results from contact with the suspended solids. Applying a mass balance over the air phase in the chamber, we have at steady state,  $N_A = \rho_{Aa}Q_a/A$ , where  $Q_a$  is the volumetric flow rate ( $\text{cm}^3/\text{s}$ ) of air through the chamber. Therefore, we can obtain the following equation for the flux to air at steady state in the grid-flux chamber

$$N_A = \left( \frac{1}{\frac{1}{K_{Aw}} + \frac{A}{Q_a H_c}} \right) \cdot \rho_{Aw} \quad (3)$$

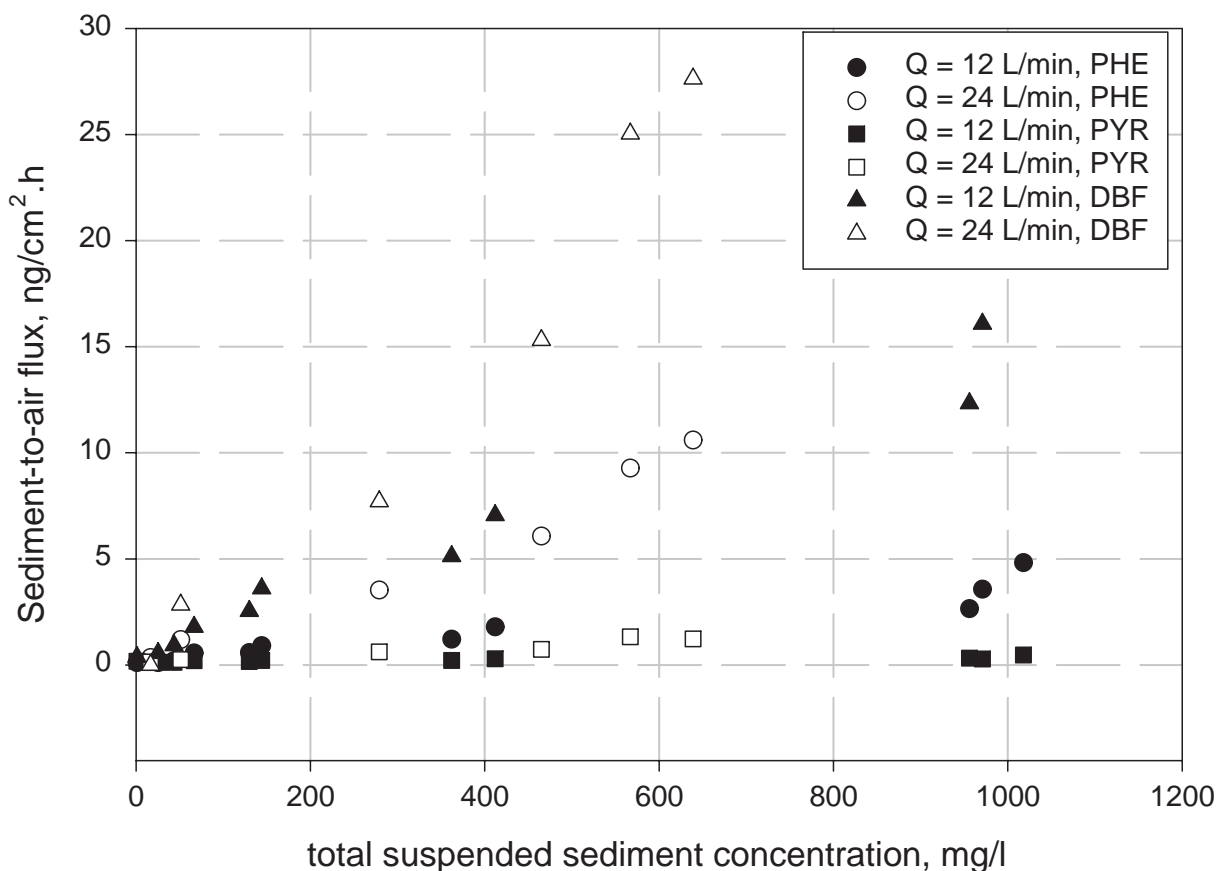


Figure 4. Sediment-to-air flux of PAHs versus suspended sediment concentration in water.

When  $K_{Aw}$  is small and  $Q_a$  is large, the transfer of PAH from water to air is mass transfer controlled. At small values of  $Q_a$ , if the air above the water column in the grid-flux chamber approaches equilibrium with the aqueous phase, then  $N_A \approx (Q_a H_C / A) \rho_{Aw}$ .

Figure 4 shows the fluxes of the three PAHs at an air flow rate of 12 L/min, i.e., an air residence time ( $\tau_{air} = V_{air} / Q_a$ ) of 2 minutes.  $V_{air}$  is the total volume of air in the chamber. This corresponded to an air velocity of 5 cm/s. Also shown in Figure 4 is the flux at a larger air flow rate of 24 L/min, where the air velocity was 35 cm/s across the air-water interface.  $\rho_{Aw}$  was measured as a function of  $\rho_s$  (or  $E_k$ ). An example plot for the low air flow rate of 12 L/min is shown in Figure 5. Increased kinetic energy at the

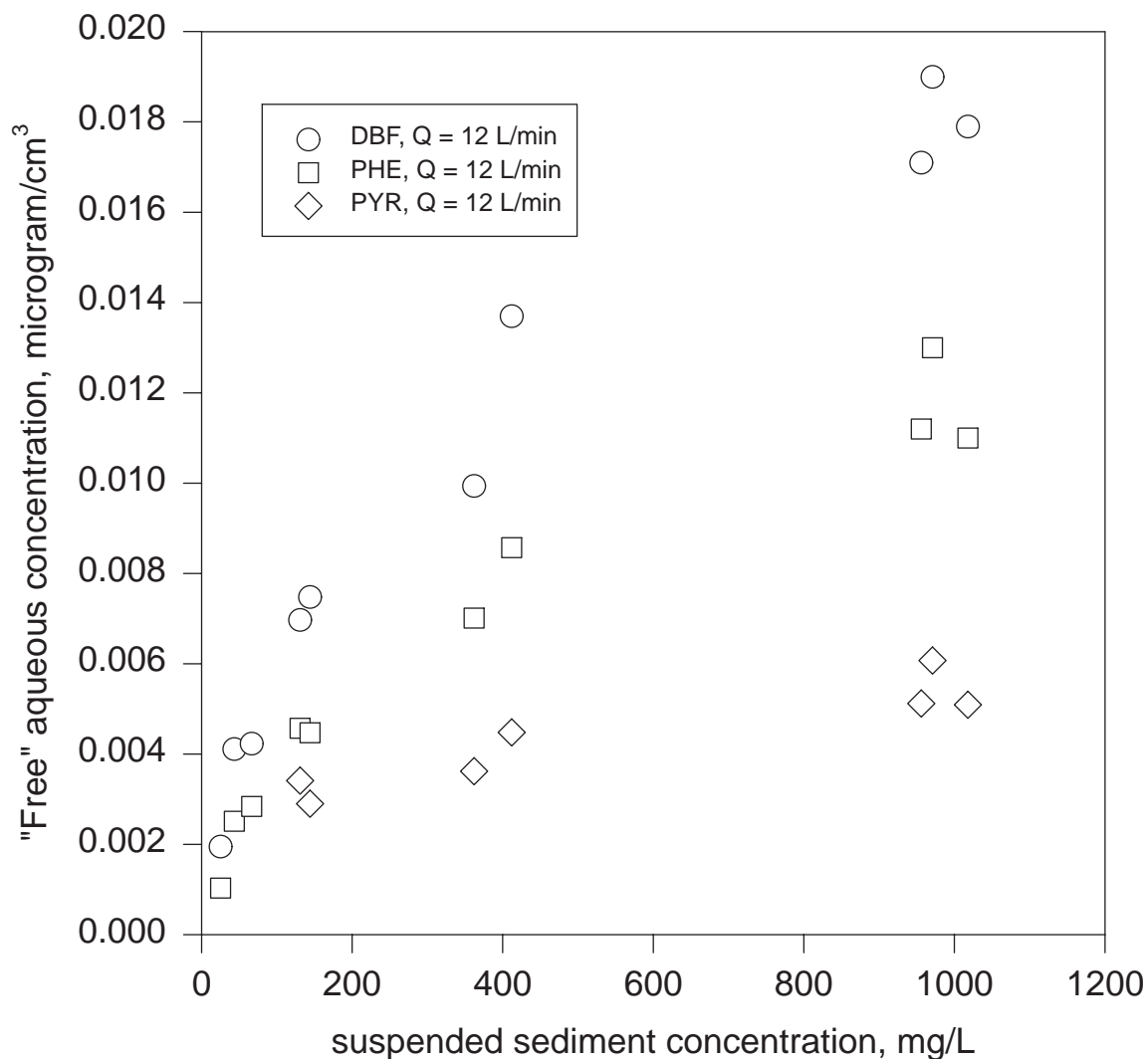


Figure 5. "Free" aqueous concentration of PAHs as a function of total suspended solids concentration.

sediment/water interface resulted in increased suspended solids in the aqueous phase which also increased the aqueous phase concentration of all three PAHs. The sediment-to-air fluxes were substantial for all the compounds studied and varied as DBF>PHE>PYR. The sediment concentrations of the three compounds were similar, hence the aqueous concentrations varied as DBF>PHE>PYR since the sediment-water partition constants were larger for DBF than PHE or PYR. The Henry's constants were in the order DBF>PHE>PYR. Therefore, the concentration driving force for volatilization was in the order DBF>PHE>PYR, and the flux was also in the same order.

From the measured fluxes and "free" aqueous concentration one can obtain the overall aqueous phase transfer coefficient using Equation (3). The values of  $K_{Aw}$  were calculated for each suspended sediment concentration (total kinetic energy). The appropriate velocity scaling factor for the liquid phase turbulence in the tank is the so-called Hopfinger-Toly velocity,  $U_{HT}$ , which is proportional to the square root of the kinetic energy,  $(E_k)^{1/2}$  [6]. A turbulent liquid phase Reynolds number can be defined as  $Re_L = 2U_{HT}L_\infty/\nu$ , where  $L_\infty$  is the longitudinal integral length scale of turbulence given by  $0.1z$  and  $\nu$  is the kinematic viscosity of water [6]. As an illustrative example, a plot of the calculated values of  $K_{Aw}$  versus  $Re_L$  for the low air flow rate of 12 L/min is given in Figure 6.  $K_{Aw}$  generally varied as DBF > PHE > PYR. Also shown in Figure 6 is the  $K_{Aw}$  value for oxygen mass transfer (a liquid phase controlled process) obtained by Chu and Jirka [6] using a grid-flux chamber of similar size. The value of  $K_{Aw}$  for PYR showed no appreciable dependence on  $Re_L$  within the small range of values investigated, whereas that for DBF and PHE slightly increased over the Reynolds number range of 100 to 300. Since, for constant air velocity, the liquid phase Reynolds number should influence only the mass transfer of compounds with appreciable liquid phase resistance, the conclusion can be drawn that for both PHE and DBF there exist a contribution of liquid phase resistance for mass transfer from water to air. In other words, the flux of PYR is independent of liquid phase turbulence; its rate is controlled by air-side resistance. The slope of  $K_{Aw}$  versus  $Re_L$  for both DBF and oxygen were similar, suggesting more liquid phase resistance for DBF than PHE.

The coefficient  $K_{Aw}$  is composed of two entities, an aqueous side mass transfer coefficient,  $k_{Aw}$ , and an air side mass transfer coefficient,  $k_{Aa}$  [16].

$$\frac{1}{K_{Aw}} = \frac{1}{k_{Aw}} + \frac{1}{k_{Aa}H_c} \quad (4)$$

$k_{Aw}$  is generally determined from oxygen mass transfer data since  $k_{Aw} \approx K_{Aw}$  for oxygen and the measurement of oxygen concentrations is standardized. Chu and Jirka [6] obtained a correlation for oxygen mass transfer coefficients in a similar grid-stirred tank for various values of  $Re_L$ . When transformed to appropriate dimensionless groups it can be used for any substance A in solution. Doing so yields

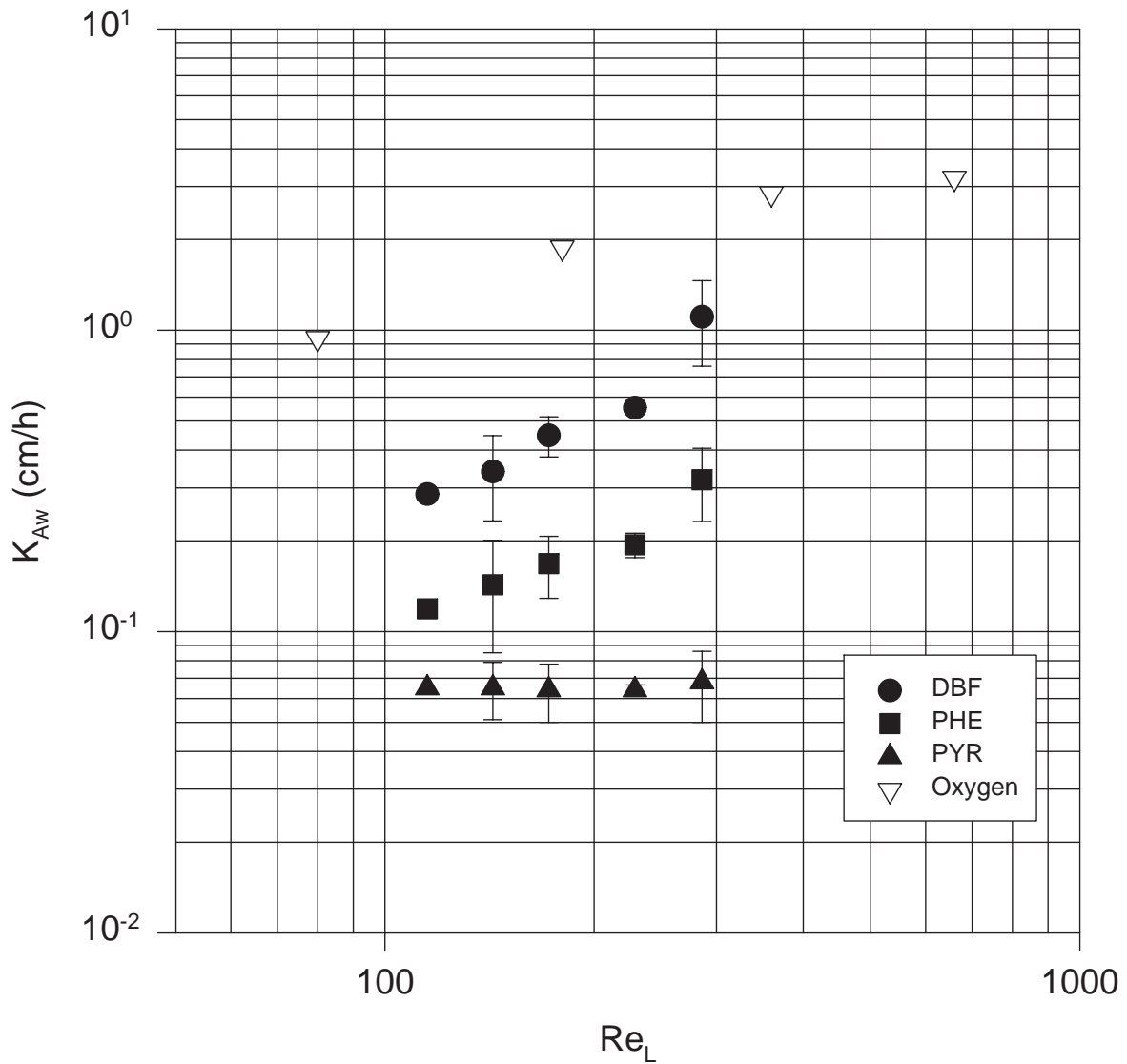


Figure 6. Overall water-phase mass transfer coefficients versus turbulent liquid phase Reynolds number. Only data for air flow rate of 12 L/min are shown. Oxygen data from Chu and Jirka [6].

$$k_{Aw} = 0.125 (\text{Re}_L \text{Sc}_{Aw})^{1/2} \frac{D_{Aw}}{L_\infty} \quad (5)$$

where  $L_\infty = 0.1 z$  and  $\text{Sc}_{Aw}$  is the Schmidt number for the SVOC in water.  $D_{Aw}$  is the corresponding molecular diffusivity of the chemical. For each value of  $\text{Re}_L$  there is a corresponding  $K_{Aw}$ . With Equation (5) used for  $k_{Aw}$ , Equation (4) can be used to extract a representative  $k_{Aa}$  for each observation shown in Figure 6. Combining the equations yields

$$k_{Aa} = \frac{1}{H_c} \left[ \frac{1}{(1/K_{Aw}) - 8L_\infty / (D_{Aw} \sqrt{\text{Re}_L \text{Sc}_{Aw}})} \right] \quad (6)$$

The value of  $k_{Aa}$  depends on the gas phase Reynolds number,  $\text{Re}_g$ , and the gas phase Schmidt number,  $\text{Sc}_g$ . Since in this experiment only a single value of  $\text{Re}_g$  was used for each experiment ( $\text{Re}_g = L \cdot v / \nu_g$  of 1302 and 9117), we can extract only an average value of  $k_{Aa}$  for each compound as shown in Table 2. Given that the reported values of Henry's constant for these compounds vary greatly [17], the values of  $k_{Aa}$  listed should only be considered as estimates of the gas phase mass transfer coefficients. A more practical and useful measure is the gas phase resistance,  $1/H_c k_{Aa}$ . From the values of  $k_{Aa}$  for each compound, one can determine the corresponding value of the gas-phase mass transfer coefficient for water,  $k_{Wa}$ , applying the correction

Table 2. Estimated values of air-phase mass transfer coefficients for SVOCs and water

Compound	$k_{Aa}$ (cm/h)		% air-side resistance	
	$\text{Re}_g = 1302$	9117	1302	9117
DBF	$240 \pm 93$	$716 \pm 477$	$68 \pm 7$	$47 \pm 7$
PHE	$209 \pm 61$	$1028 \pm 443$	$88 \pm 4$	$71 \pm 10$
PYR	$153 \pm 26$	$769 \pm 165$	$96 \pm 1$	$88 \pm 5$
Water	$634 \pm 93$	$2665 \pm 528$	100	100

Note:  $\text{Re}_g$  is defined as  $L \cdot V / \nu_g$ , where  $L$  is the air flow path length,  $V$  is the air flow velocity and  $\nu_g$  is the kinematic viscosity of air.  $V = 5$  cm/s and  $35$  cm/s respectively for  $\text{Re}_g$  of 1302 and 9117 obtained by direct measurement within the grid-flux chamber.

for diffusivity [16]. The average value so obtained is also shown in Table 2.

As noted in Figure 4, the flux to air upon resuspension was found to increase when the air flow velocity over the water column in the chamber increased from 5 cm/s (at 12 L/min) to 35 cm/s (at 24 L/min). At the increased air velocity the air boundary layer thickness is decreased and hence the rate of transport from water to air is enhanced. The mass transfer coefficients for the three compounds were observed to be larger at the higher air flow velocity as shown in Table 2.

From the values of individual gas phase mass transfer coefficients for the compounds, one can also obtain the gas phase mass transfer coefficient for water evaporation by scaling the values to the appropriate ratios of molecular weights. These values are also shown in Table 2 for comparison. The gas phase transfer coefficient for water evaporation increased from 634 cm/h at a  $Re_g$  of 1302 to 2665 cm/h at a  $Re_g$  of 9117. In the natural environment, under turbulent conditions, the gas phase mass transfer coefficient for water evaporation is reported to be in the range 500 to 3,000 cm/h [16].

As shown in Table 2, the average gas phase resistance of the compounds is significant and indicates that in estimating the volatilization of SVOCs, gas-phase resistance cannot be neglected. Therefore, it is improper to scale the overall mass transfer coefficients for SVOCs directly from the oxygen transfer data, as is usually done for most volatile contaminants.

In a CDF, during the filling stages when resuspension is the greatest, the air emissions will also be substantial. However, since the particles will be of diverse sizes, their settling velocities will vary and the residence times of particulates will differ according to particle size. Correspondingly, the concentration of contaminant “available” for volatilization from the aqueous phase will vary as particle concentration changes. As large particulates settle to the bottom, the air emission will decrease until a degree of constant resuspension due to small particulates is realized. At this time, the air emission flux will be sustained so long as there is a large concentration gradient for the chemical between the aqueous phase and atmospheric boundary layer. Fortunately, in the present design of the apparatus the particle size was kept constant due to the oscillating grid mechanism. The time varying effects due to diverse particulate sizes will have to be simulated in the apparatus to study the variation in flux due to resuspension in an actual CDF. Experiments will have to be performed to ascertain the value of  $K_{Aw}$  as a function of air velocity near the air/water interface, since it is the predominant variable affecting the mass transfer coefficient in a field situation. These and other aspects are being pursued in our laboratory.

## CONCLUSIONS

The following conclusions can be drawn from this work:

- Sediment resuspension in a grid-flux chamber was related to the turbulence near the sediment-water interface which was characterized by the Hopfinger-Toly relationship.
- The flux of the SVOCs to the air was measured at various suspended sediment concentrations and was found to vary in the order dibenzofuran > phenanthrene > pyrene.
- The flux increased with increasing suspended sediment concentration in water, increasing Henry's constant and decreasing sediment/water partition constant for the chemical.
- The overall mass transfer coefficients showed significant air phase resistance for the SVOCs.

## ACKNOWLEDGMENTS

This research was supported by a grant from the U S Environmental Protection Agency through the Hazardous Substance Research Center (South and Southwest) at LSU. It has not been subject to the required EPA peer review and does not necessarily reflect the views of the Agency. We thank Dr. Alexander Kochetkov for assistance with the analyses of samples.

## REFERENCES

1. Valsaraj, K. T., Thibodeaux, L. J. and Reible, D. D., "Modeling air emissions from contaminated sediment dredged materials", in Dredging, Remediation and Containment of Contaminated Sediments, ASTM STP 1293, K. R. Demars, G. N. Richardson, R. N. Yong and R. C. Chaney (Eds.), American Society for Testing and Materials, Philadelphia, 1995, pp. 227-238.
2. Virag, P, Feick, N, Hanes, D., Beaudoin, M. and L'Heureux, P., Ambient air monitoring for PCBs at the New Bedford Harbor Superfund site, Paper No: 96-TP40.07, 89<sup>th</sup> Annual Meeting and Exhibition of Air and Waste Management Association, Nashville, TN, 1996.
3. van Oostrum, R. W, and Vroege, Ir. P., "Turbidity and contaminant release during dredging of contaminated sediments", in Dredging '94 Volume 1, E. Clark McNair, Jr., (Ed.), American Society of Civil Engineers, New York, NY, 1994, pp. 210-219.
4. Thompson, S. M. and Turner, J. S., Mixing across an interface due to turbulence generated by an

- oscillating grid, *J. Fluid Mech.*, 67 (1975) 349.
5. Hopfinger, E. J. and Toly, J. A., Spatial decaying turbulence and its relation to mixing across density interfaces, *J. Fluid Mech.*, 78 (1976) 155.
  6. Chu, C. R. and Jirka, G. H., Turbulent gas flux measurements below the air-water interface of a grid-stirred tank, *Int. J. Heat Mass Transfer*, 35 (1992) 1957.
  7. Tsai, C. H. and Lick, W., A portable device for measuring sediment resuspension, *J. Great Lakes Res.*, 12 (1986) 314.
  8. Huppert, H. E., Turner, J. S. and Hallworth, M. A., Sedimentation and entrainment in dense layers of suspended particles stirred by an oscillating grid, *J. Fluid Mech.*, 289 (1995) 263.
  9. Connolly, J. P., Armstrong, N. E. and Miksad, R. W., Adsorption of hydrophobic pollutants in estuaries, *J. Environ. Eng. (ASCE)*, 109 (1983) 17.
  10. Thoma, G. J., Ph.D. Dissertation, Louisiana State University, Baton Rouge, LA (1994).
  11. Standard Methods for the Examination of Water and Wastewater, 18<sup>th</sup> Ed., American Public Health Association, Washington, D.C. (1992).
  12. U. S. EPA, Test Methods for Evaluating Solid Waste - Physical and Chemical Methods, SW-846, Second Edition, NTIS, Springfield, VA (1982).
  13. Orlins, J. J., Construction and Calibration of a Sediment Resuspension and Chemical Flux Chamber Driven by an Oscillating Grid, Interim Report to the EPA Hazardous Substance Research Center (South and Southwest), LSU, Baton Rouge, LA (1996).
  14. Borglin, S., Wilke, A., Jepsen, R. and Lick, W., Parameters affecting the desorption of hydrophobic organic chemicals from suspended sediments, *Environ. Toxicol. Chem.*, 15 (1996) 2254.
  15. DeSilva, I. P. D. and Fernando, H. J. S., Some aspects of mixing in a stratified turbulent patch, *J. Fluid Mech.*, 240 (1992) 601.
  16. Thibodeaux, L. J., Environmental Chemodynamics, Second Edition, John Wiley & Sons, Inc., New York, NY (1996).
  17. Valsaraj, K. T., Elements of Environmental Engineering - Thermodynamics and Kinetics, CRC Press, Boca Raton, FL (1995).